compartments at baseline and follow-up using the BLOKS scoring system. Two musculoskeletal radiologists read the images in pairs blinded to the time point of acquisition. A 3D inversion recovery-prepared SPGR sequence 90 minutes after intravenous gadolinium injection was acquired for dGEMRIC assessment. Tibiofemoral cartilage from baseline and follow-up MRIs was segmented by a trained fellow who was blinded to the time point of acquisition. According to changes in dGEMRIC indices from baseline to follow-up, three groups were defined: decrease (regions exhibiting any decrease of dGEMRIC), stable (regions exhibiting stable indices), and increase dGEMRIC (regions exhibiting any increase of dGEMRIC). Regarding changes of cartilage morphology from baseline to follow-up, three groups were defined: worsening (regions exhibiting any increase in BLOKS score – cartilage loss), stable (regions with stable BLOKS scores) and improvement (regions exhibiting any decrease in BLOKS score). A decrease in dGEMRIC indices (decrease dGEMRIC group) over one year was considered as the predictor of cartilage loss. Co-variance analysis was performed to determine if baseline dGEMRIC indices were different between regions with vs. without cartilage loss. The association of any decrease in dGEMRIC indices from baseline to follow-up with cartilage loss in the same region was assessed using logistic regression. In addition we used the maximal statistical approach to determine at which cut-off value baseline dGEMRIC would be most predictive for cartilage loss after one year.

Results: A total of 434 regions from 140 knees were included: 25 (5.8%) had cartilage loss over one year and 408 (92.2%) did not. Furthermore, 153 (35.3%) regions had a decrease in dGEMRIC indices over one year and 280 (64.7%) did not. The mean baseline dGEMRIC index at the lateral tibia was significantly lower for regions exhibiting cartilage loss over one year compared to regions without cartilage loss (484.7 ± 63.9 vs. 649.1 ± 140.7; p=0.04). However, only 3 lateral tibial regions exhibited cartilage loss over one year. No significant differences in mean baseline dGEMRIC were found in other tibiofemoral regions (Table 1). No significant associations between a decrease in dGEMRIC indices over time and cartilage loss were observed (Table 2). A cut-off value of baseline dGEMRIC predicting cartilage loss could not be established.

Conclusions: The association between a decrease in dGEMRIC over time and cartilage loss in the tibiofemoral compartments over one year could not be demonstrated in this sample of middle-aged women. Low numbers of regions exhibiting cartilage loss and the challenge of definition of change in dGEMRIC indices over time may have contributed to these findings. The monitoring of changes in dGEMRIC indices over time still need to be validated before it can be applied as an imaging biomarker for longitudinal cartilage loss.

Table 1
Differences in the mean baseline dGEMRIC indices in regions with progression of cartilage loss vs. regions without progression of cartilage loss over one year. MF = medial femur; MT = medial tibia; LF = lateral femur; LT = lateral tibia; BL = baseline; FU = 1 year follow-up; SD = standard deviation.

Regions	Cartilage loss from BL to FU	Baseline dGEMRIC		p-value
		N	Mean (SD)	
MF	With cartilage loss (N=16)	15	587.80 (114.23)	0.76
	Without cartilage loss (N=95)	94	597.54 (112.26)	
MT	With cartilage loss (N=3)	3	518.33 (111.42)	0.35
	Without cartilage loss (N=109)	100	573.60 (99.45)	
LF	With cartilage loss (N=4)	4	579.25 (98.39)	0.93
	Without cartilage loss (N=106)	106	584.31 (115.10)	
LT	With cartilage loss (N=3)	3	484.67 (63.89)	**0.046***
	Without cartilage loss (N=109)	109	649.05 (140.67)	

Table 2
The associations of changes in dGEMRIC indices and progression of cartilage loss over one year. *Adjusted for age, body mass index, and Kellgren-Lawrence grade of radiographic OA. MF = medial femur; MT = medial tibia; LF = lateral femur; LT = lateral tibia; BL = baseline; FU = one year follow-up; OR = odds ratio; CI = confidence intervals.

Region	dGEMRIC changes (from BL to FU)	Cartilage loss (from BL to FU)		Crude OR (95% CI)	Adjusted OR* (95% CI)
		Absence	Presence		
MF	Stable or increase	53 (83%)	11 (17%)	1.0 (ref)	1.0 (ref)
	Any decrease	38 (90%)	4 (10%)	0.5 (0.2, 1.7)	0.5 (0.1, 1.8)
MT	Stable or increase	59 (97%)	2 (3%)	1.0 (ref)	1.0 (ref)
	Any decrease	35 (97%)	1(3%)	0.8 (0.1, 9.6)	1.1 (0.1, 16.2)
LF	Stable or increase	71 (96%)	3 (4%)	1.0 (ref)	1.0 (ref)
	Any decrease	35 (97%)	1 (3%)	0.7 (0.1, 6.7)	0.6 (0.1, 6.7)
LT	Stable or increase	70 (96%)	3 (4%)	1.0 (ref)	1.0 (ref)
	Any decrease	39 (100%)	0	-	-

371
LONGTERM PROFESSIONAL ATHLETIC ACTIVITY RESULTS IN INCREASED STRUCTURAL KNEE JOINT SYNOVIAL TISSUE PATHOLOGY

H. Boeth †, F. Eckstein ‡, G. Diederichs §, A. Schlausch †, W. Wirth ‡, G.N. Duda †. † *Julius Wolff Inst., Berlin, Germany;* ‡ *Inst. of Anatomy, Paracelsus Med. Univ., Salzburg, Austria;* § *Dept. of Radiology, Charité – Univ.smedizin Berlin, Berlin, Germany*

Purpose: The aim of this study was to analyze the presence of structural synovial tissue pathology by magnetic resonance imaging (MRI), in young and mature volleyball athletes, and its longitudinal change over 2 years. These observations were compared with previously reported prevalence rates in population-based studies.

Methods: Eighteen adolescent (8 male, 10 female, baseline age 16.0±0.8y) and 18 mature (9 male, 9 female, 46.8±5.1y) professional volleyball athletes were studied. MR images (Coronal PD FS, Sagital 3D VIBE, Axial T2 MEDIC) were acquired at baseline (BL) and at 2 year follow-up (FU). From the 14 features of the WORMS scoring system, cartilage signal and morphology, medial and lateral meniscal integrity, and osteophytes were evaluated, and combined to compute a "total" WOMRS score. These scores were derived for the medial femoro-tibial joint (MFTJ), lateral femoro-tibial joint (LFTJ), patello-femoral joint (PFJ), and the total knee joint. Post-hoc tests were conducted to test for statistical significances between the cohorts, as well as paired T-tests to examine differences from BL to FU.

Results: Mature athletes showed a greater prevalence of cartilage and meniscus lesions and osteophytes, resulting in a statistically greater total WORMS score compared to the adolescent athletes (baseline: adolescent athletes: 4.7 ± 4.6; mature athletes: 34.6 ± 30,6; follow-up: 6.7 ± 5.6 and 40.9 ± 30.3, respectively) (Figure 1, P <0.001). While the adolescent athletes did not possess any incidence of cartilage pathology neither at BL nor FU, the mature athletes show an increase from 7.6±9.5 at BL to 10.1±10.9 at FU (P=0.012) in the total knee joint with the greatest changes occurring in the LFTJ. Table 1 presents the findings in the menisci that are increased in the medial, lateral as well as total knee joint. Already within the 2 year follow-up period, the formation of osteophytes increased statistically significantly from 3.9 ± 2.9 at BL to 5.8 ± 3.4 at FU in adolescent athletes (P <0.01). A similar increase was found in mature athletes, however from an elevated baseline level (from 23.2 ± 15.7 at BL to 26.1 ± 15.8 at FU; P <0.001). The total WORMS score increased from BL to FU in both cohorts (P<0.01 for adolescent athletes).

Conclusions: These MRI-based findings indicate towards a significant change in structural tissue pathology due to athletic activity in the long-term as well as already within a 2 year follow-up time. These changes were of similar magnitude in adolescent and mature subjects, although mature athletes started from substantially higher baseline values. The comparison of the above WORMS scores and features with those published in the literature shows that the values of the mature athletes fall between those reported in healthy controls and osteoarthritic cohorts. Additionally, other studies that investigated in patients with knee joint problems show a trend to higher values in comparison to the values of the mature athletes presented here. As anticipated, the values for the adolescent athletes are much lower and not comparable to the other

Mean score ± STD, differentiated into medial, lateral and total menisci at BL and FU

	Medial		Lateral		Total		
	BL	FU	BL	FU	BL	FU	P-value
Adolescent athletes	0.3 ± 0.5	0.3 ± 0.6	0.0 ± 0.0	0.1 ± 0.5	0.3 ± 0.5	0.4 ± 0.9	0.187
Mature athletes	1.1 ± 1.3	1.2 ± 1.4	0.8 ± 1.6	0.9 ± 1.6	1.9 ± 2.3	2.1 ± 2.3	0.042

cohorts as they are neither age nor BMI matched, however, the increase within 2 years of MRI-based signs of osteophytes and meniscal lesions is remarkable. Even though the level is well below any pathology in the adolescent athletes, the findings of this study indicates that high frequency training in competitive sports like volleyball show already within two years significant signs of structural tissue pathologies. These pathologies increase substantially over time to levels well above of intact control knees but below those of osteoarthritis patients.

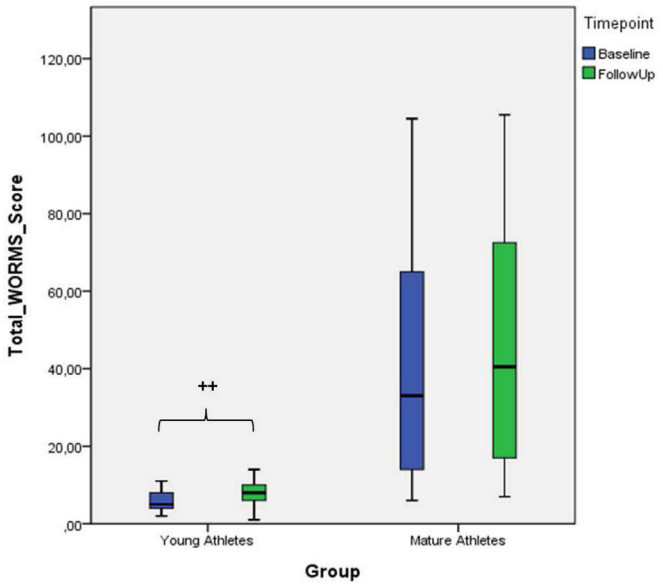

372
INVESTIGATING THE ROLE OF BONE MICROARCHITECTURE IN EARLY OSTEOARTHRITIS USING NEW IN VIVO 3D HIGH-RESOLUTION PERIPHERAL QUANTITATIVE COMPUTED TOMOGRAPHY

A. Kroker, S.L. Manske, Y. Zhu, S.K. Boyd. *Univ. of Calgary, Calgary, AB, Canada*

Purpose: The sequence of events leading to osteoarthritis (OA) after joint injury such as an acute anterior cruciate ligament (ACL) tear is poorly understood. Increasing evidence suggests that subchondral bone plays an important role, and may even precede cartilage loss. However, the nature of the bone changes that may be linked to OA progression is unclear as both high and low bone mineral density (BMD) has been associated with radiographic OA. To date, in vivo x-ray bone assessment in the human knee includes radiography, 3D quantitative computed tomography (QCT) at resolutions of 500 μm or larger. Magnetic resonance imaging (MRI) provides excellent visualization and quantification of soft tissues such as cartilage, but is less suited to detect bone microarchitectural changes. Recently, high-resolution peripheral QCT (HR-pQCT) scanners have been employed to assess bone microarchitecture in peripheral limbs. The new development of the second generation scanner (XtremeCTII, Scanco Medical) with a larger field of view (FOV, 14 cm), longer gantry (115 cm), and increased scan length (20 cm) allows examination of skeletal sites such as the knee and elbow. The purpose of this study was to establish a technique for measuring in vivo bone microarchitecture in human knees, with and without ACL reconstruction (ACLR), using HR-pQCT.
Methods: To perform bone microarchitectural assessments of the knee by HR-pQCT, we designed a restraint to statically support the knee in the scanner FOV. We established a scanning protocol (61 μm voxel size, 100 ms integration time, 900 projections/180 degree) to acquire a 6 cm long region of interest (ROI) that includes approximately 2 cm of the proximal tibia and 4 cm of the distal femur. We scanned 5 individuals with no history of knee joint injury and 4 with a knee injury (1 OA patient; 3 with ACLR 6 months to 15 years prior). Visualization and trabecular bone assessment was performed after data was Gaussian filtered and thresholded (475 mg HA/ccm) to segment bone from soft tissue. We performed virtual biopsies (125 cmm) to examine trabecular bone volume fraction, number, thickness and separation in the medial and lateral tibial plateaus of the injured and non-injured knees. We examined the peri-tunnel BMD (mg HA/ccm) in the ACLR knees.
Results: Using our device, we were able to position 8 of 9 participants fully in the FOV (The femur girth of one ACL-repaired participant was wide (44 cm) and some soft tissue was outside the FOV). Total scan time for a 6 cm ROI is 25 min, which will be reduced in the near future with manufacturer's modifications. The scans generated ~8 GB grey-scale data sets and ~ 50 MB segmented data sets.
Trabecular microarchitecture was resolved in all scans (Fig 1). There were no apparent differences in trabecular microarchitecture between injured and contralateral tibiae. Unlike the OA knee, none of the ACLR knees exhibited degenerative signs. We could clearly visualize the tibial tunnel (Fig 2) and the distal end of the femoral tunnel(s) in all 3 ACLR participants. The peri-tunnel surface was more dense (mean = 575 mg HA/ccm) than the adjacent trabecular region (mean = 168 mg HA/ccm) and increased with time since ACL-repair (515 mg HA/ccm after 6 months vs. 626 mg HA/ccm after 15 years).
Conclusions: We have performed the first high-resolution (61 μm) bone microarchitectural measurements at the human knee in vivo. While our focus was on assessing bone, we noted that cartilage provided significant contrast in regions of the knee joint suggesting it may be possible to examine further. Our future work will expand our cohort and standardize post-processing techniques to automatically define medial and lateral compartments, as well as perform analysis as a function of depth from the cartilage surface. Our goal is to characterize microarchitectural bone changes, including bone marrow lesions, that may be associated with the detection and progression of osteoarthritis.

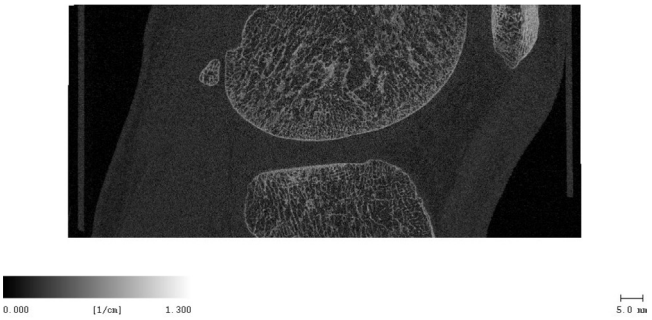

Fig 1. Sagittal HR-pQCT image of the knee joint in a participant with an ACL reconstruction.

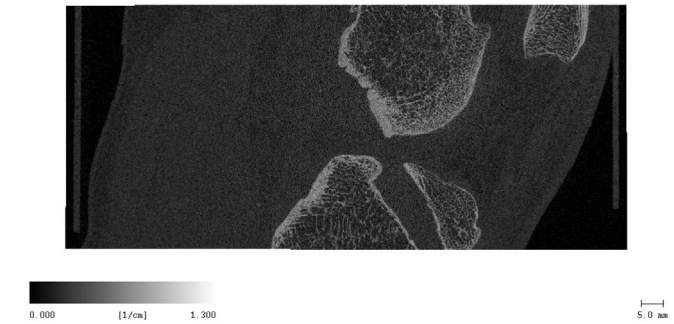

Fig 2. Sagittal HR-pQCT of the tibial tunnel in a participant with an ACL reconstruction.

373
DETECTION OF EXTREMELY EARLY GRADE OSTEOARTHRITIS OF THE KNEE BY ULTRASONOGRAPHY

N. Kumahashi, S. Kuwata, M. Masaru Kadowaki, H. Takuwa, Y. Uchio. *Shimane Univ., Izumo-shi, Japan*

Purpose: Early diagnosis of osteoarthritis (OA) of the knee is essential to prevent further cartilage destruction and to avoid surgery. The aims of this study were to evaluate the quality of cartilage in the femoral condyle of the knee, to clarify the relationship between echoic findings, OA symptoms and muscle power, and to determine the effectiveness of ultrasonography to diagnose early OA in the knee.
Methods: We enrolled 973 Japanese volunteers (322 men and 651 women; mean age = 72 years; age range: 41-93 years). They received